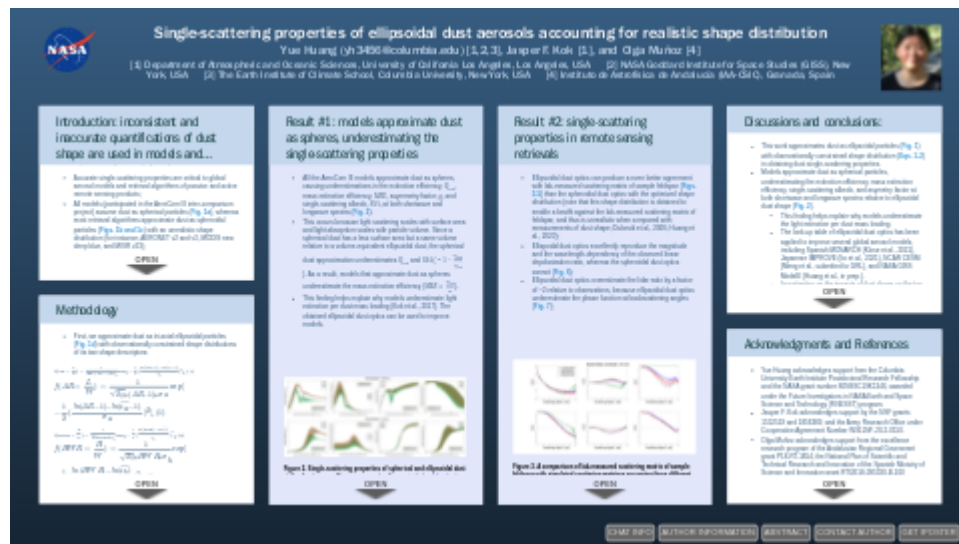


# Single-scattering properties of ellipsoidal dust aerosols accounting for realistic shape distribution




**Yue Huang (yh3456@columbia.edu) [1,2,3], Jasper F. Kok [1], and Olga Muñoz [4]**

[1] Department of Atmospheric and Oceanic Sciences, University of California Los Angeles, Los Angeles, USA [2] NASA Goddard Institute for Space Studies (GISS), New York, USA [3] The Earth Institute of Climate School, Columbia University, New York, USA [4] Instituto de Astrofísica de Andalucía (IAA-CSIC), Granada, Spain



**PRESENTED AT:**



**AGU FALL MEETING**  
New Orleans, LA & Online Everywhere  
13–17 December 2021

Poster Gallery  
brought to you by  
**WILEY**

# INTRODUCTION: INCONSISTENT AND INACCURATE QUANTIFICATIONS OF DUST SHAPE ARE USED IN MODELS AND REMOTE SENSING RETRIEVALS

- Accurate single-scattering properties are critical to global aerosol models and retrieval algorithms of passive and active remote sensing products;
- All models (participated in the AeroCom III inter-comparison project) assume dust as spherical particles (**Fig. 1a**), whereas most retrieval algorithms approximate dust as spheroidal particles (**Figs. 1b and 1c**) with an unrealistic shape distribution (for instance, AERONET v2 and v3, MODIS new deep blue, and MISR v23);
- A recent study (Huang et al., 2020 (<https://agupubs.onlinelibrary.wiley.com/doi/full/10.1029/2019GL086592>)) found that dust shape deviates substantially from spheres and spheroids, and that models and retrieval algorithms underestimate dust asphericity by a factor of ~3 to 5;
- The inconsistent and inaccurate dust shape assumptions in models and retrieval algorithms generate bias in the dust single-scattering properties that further propagate into the estimated dust distributions and dust impacts;
- Here, we approximate dust as tri-axial ellipsoidal particles (**Fig. 1d**) with observationally constrained shape distributions (Huang et al., 2020 (<https://agupubs.onlinelibrary.wiley.com/doi/full/10.1029/2019GL086592>)) in obtaining dust single-scattering properties at both shortwave and longwave spectra.

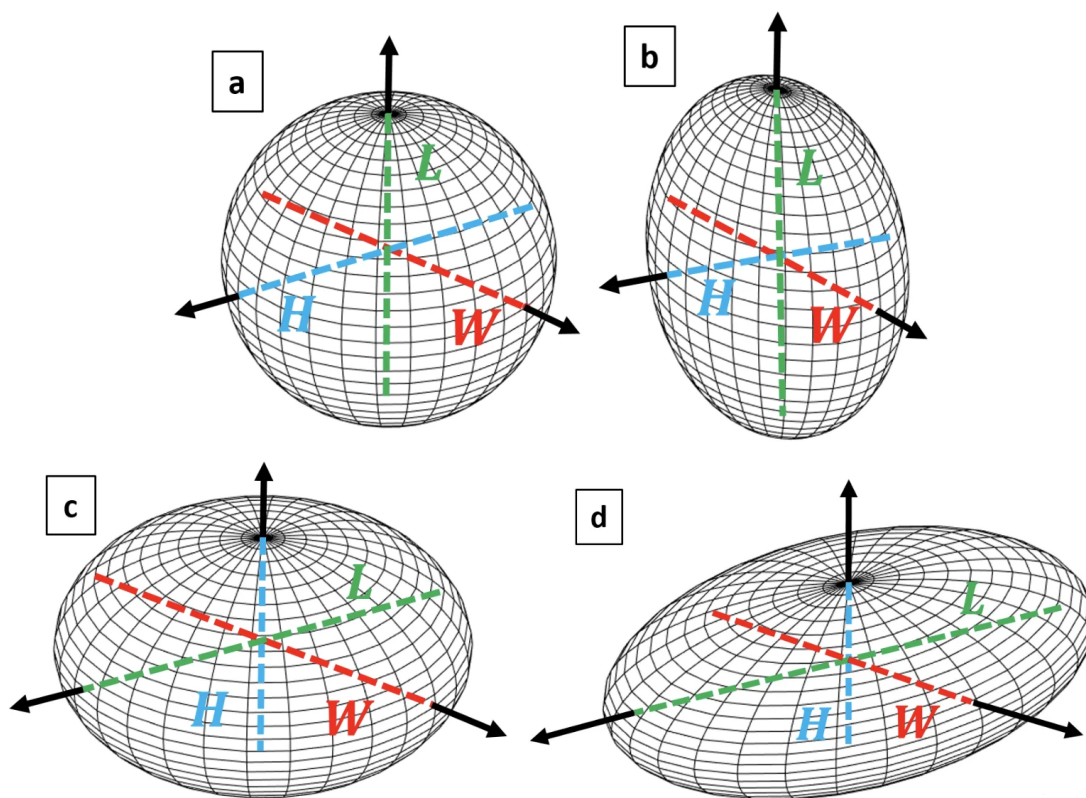


**Figure 1.** Three-dimensional view of a dust particle approximated as (a) a sphere, (b) prolate spheroid, (c) oblate spheroid, and (d) tri-axial ellipsoid. In each plot, the three perpendicular axes are denoted. The largest, intermediate, and smallest axes are referred to as particle length,  $L$ , particle width,  $W$ , and height  $H$ , respectively. In shape (a)  $L = W = H$ , in shape (b)  $L \geq W = H$ , in shape (c)  $L = W \geq H$ , and in shape (d)  $L \geq W \geq H$ , such that, to quantify dust

asphericity, shape (a) does not need a shape descriptor, shapes (b) and (c) need one shape descriptor (i.e., aspect ratio  $\frac{L}{H}$ ), and shape (d) needs two shape descriptors (i.e., aspect ratio  $\frac{L}{W}$  and height-to-width ratio  $\frac{H}{W}$ ). Note that v2 and v3 inversion algorithms of AERONET assume that dust particles are spheroidal and assume an equal presence of prolate and oblate spheroids with the same aspect ratio (Dubovik et al., 2006).

## METHODOLOGY

- First, we approximate dust as tri-axial ellipsoidal particles (**Fig. 1d**) with observationally constrained shape distributions of its two shape descriptors:

$$f\left(AR = \frac{L}{W}\right) = \frac{1}{\sqrt{2\pi} * (AR-1) * \sigma_a} \exp\left[-\frac{1}{2} \left(\frac{\ln(AR-1) - \ln(\overline{\epsilon_a}-1)}{\sigma_a}\right)^2\right], (1)$$

$$f\left(HWR = \frac{H}{W}\right) = \frac{1}{\sqrt{2\pi} * HWR * \sigma_h} \exp\left[-\frac{1}{2} \left(\frac{\ln(HWR) - \ln(\overline{\epsilon_h})}{\sigma_h}\right)^2\right], (2)$$

where  $\sigma_a = 1.73 \pm 0.03$ ,  $\overline{\epsilon_a} = 0.70 \pm 0.02$ ,  $\sigma_h = 0.40 \pm 0.07$ , and  $\overline{\epsilon_h} = 0.73 \pm 0.09$  at a global scale (Huang et al., 2020);

- Second, we combine the shape distributions (**Eqs. 1 and 2**) with a database of the single-scattering properties of tri-axial ellipsoidal dust particles (Meng et al., 2010) to obtain shape-integrated dust single-scattering properties that are resolved by size, wavelength, and refractive index;
- Third, the obtained single-scattering properties are validated against the laboratory and field measurements of the scattering matrix, the linear depolarization ratio, and the lidar ratio.

# RESULT #1: MODELS APPROXIMATE DUST AS SPHERES, UNDERESTIMATING THE SINGLE-SCATTERING PROPERTIES

- All the AeroCom III models approximate dust as spheres, causing underestimations in the extinction efficiency,  $Q_{ext}$ , mass extinction efficiency,  $MEE$ , asymmetry factor,  $g$ , and single-scattering albedo,  $SSA$ , at both shortwave and longwave spectra (Fig. 2).
- This occurs because light scattering scales with surface area and light absorption scales with particle volume. Since a spherical dust has a less surface area but a same volume relative to a volume-equivalent ellipsoidal dust, the spherical dust approximation underestimates  $Q_{ext}$  and  $SSA (= 1 - \frac{Q_{abs}}{Q_{ext}})$ . As a result, models that approximate dust as spheres underestimate the mass extinction efficiency ( $MEE \propto \frac{Q_{ext}}{D}$ ).
- This finding helps explain why models underestimate light extinction per dust mass loading (Kok et al., 2017). The obtained ellipsoidal dust optics can be used to improve models.

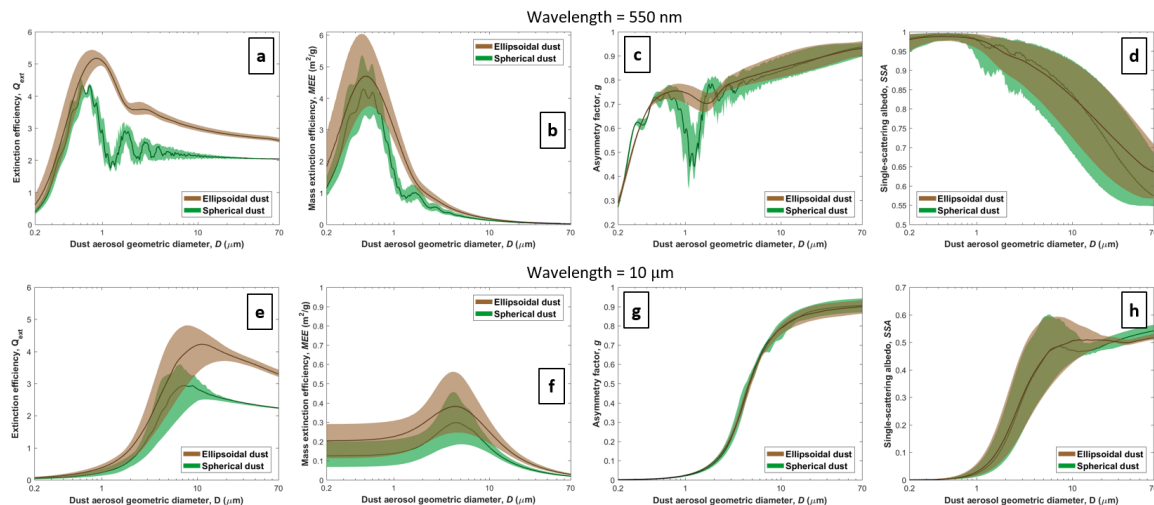


**Figure 2. Single-scattering properties of spherical and ellipsoidal dust at the shortwave and longwave spectra.** Top row includes: (a) extinction efficiency,  $Q_{ext}$ , (b) mass extinction efficiency,  $MEE$ , (c) asymmetry factor,  $g$ , and (d) single-scattering albedo,  $SSA$ , at a wavelength of 550 nm. Bottom row includes: (e)  $Q_{ext}$ , (f)  $MEE$ , (g)  $g$ , and (h)  $SSA$  at a wavelength of 10  $\mu m$ . The refractive index of dust aerosols is  $1.53 \pm 0.03 - 10^{-2.75 \pm 0.25} * i$  at 550 nm converging the ranges of Kok et al. (2017) and Di Biagio et al. (2019), and it is  $1.70 \pm 0.2 - 10^{-0.40 \pm 0.11} * i$  at 10  $\mu m$  converging the ranges of Volz (1972), Volz (1973), Hess et al. (1988), and Di Biagio et al. (2017). In each of the eight plots, the central lines denote the medians, and the shaded ranges denote the 95% confidence intervals.

## RESULT #2: SINGLE-SCATTERING PROPERTIES IN REMOTE SENSING RETRIEVALS

- Ellipsoidal dust optics can produce a even better agreement with lab-measured scattering matrix of sample feldspar (**Figs. 3-5**) than the spheroidal dust optics with the optimized shape distribution (note that this shape distribution is obtained to enable a bestfit against the lab-measured scattering matrix of feldspar, and thus is unrealistic when compared with measurements of dust shape; Dubovik et al., 2006; Huang et al., 2020);
- Ellispodal dust optics excellently reproduce the magnitude and the wavelength-dependency of the observed linear depolarization ratio, whereas the spheroidal dust optics cannot (**Fig. 6**);
- Ellipsoidal dust optics overestimate the lidar ratio by a factor of ~2 relative to observations, because ellipsoidal dust optics underestimate the phase function at backscattering angles (**Fig. 7**);

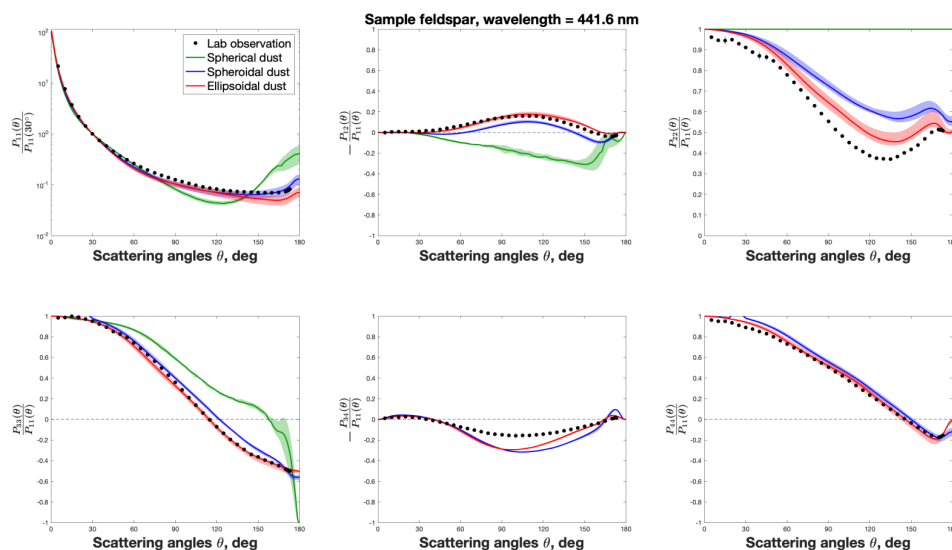


**Figure 3. A comparison of lab-measured scattering matrix of sample feldspar with simulated scattering matrices assuming three different dust shapes at wavelength of 441.6 nm.** The shaded ranges denote uncertainties from the dust refractive index. The size distribution of the three simulations is taken as the lab-measured size distribution of feldspar that was measured simultaneously as the measured scattering matrix (Volten et al., 2001; Munoz et al., 2012). The shape distribution of ellipsoidal dust optics comes from observational constraints (aka, [Eqs 1 and 2](#)). The shape distribution of spheroidal dust optics comes from Dubovik et al. (2006), which is obtained to enable a bestfit against the lab-measured scattering matrix of feldspar. Here, the ellipsoidal dust optics can produce a even better agreement with lab-measured scattering matrix than the spheroidal dust optics with optimized shape distribution.

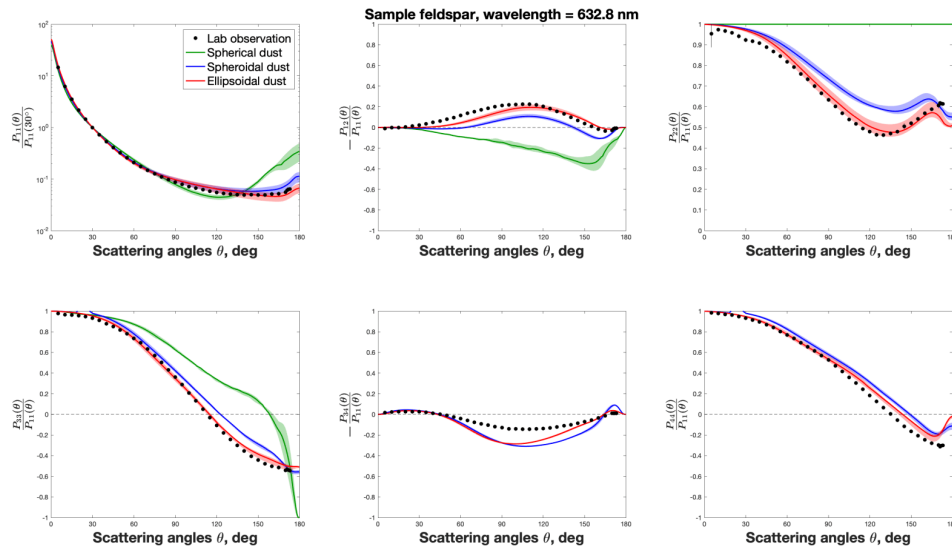


Figure 4. Similar to Fig 3 but at a different wavelength of 632.8 nm.

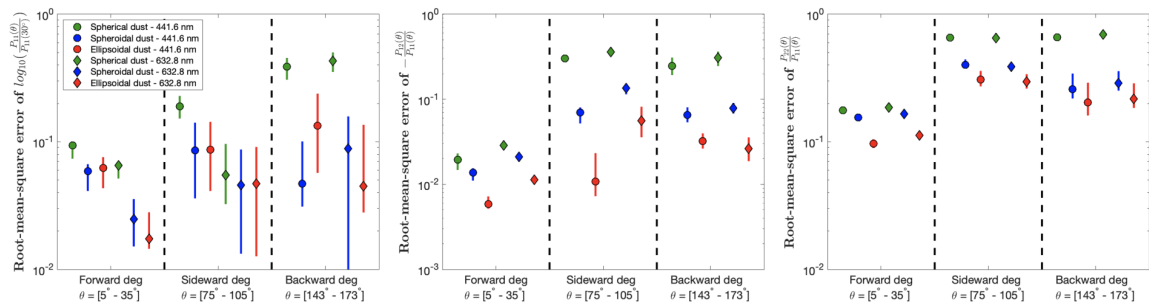
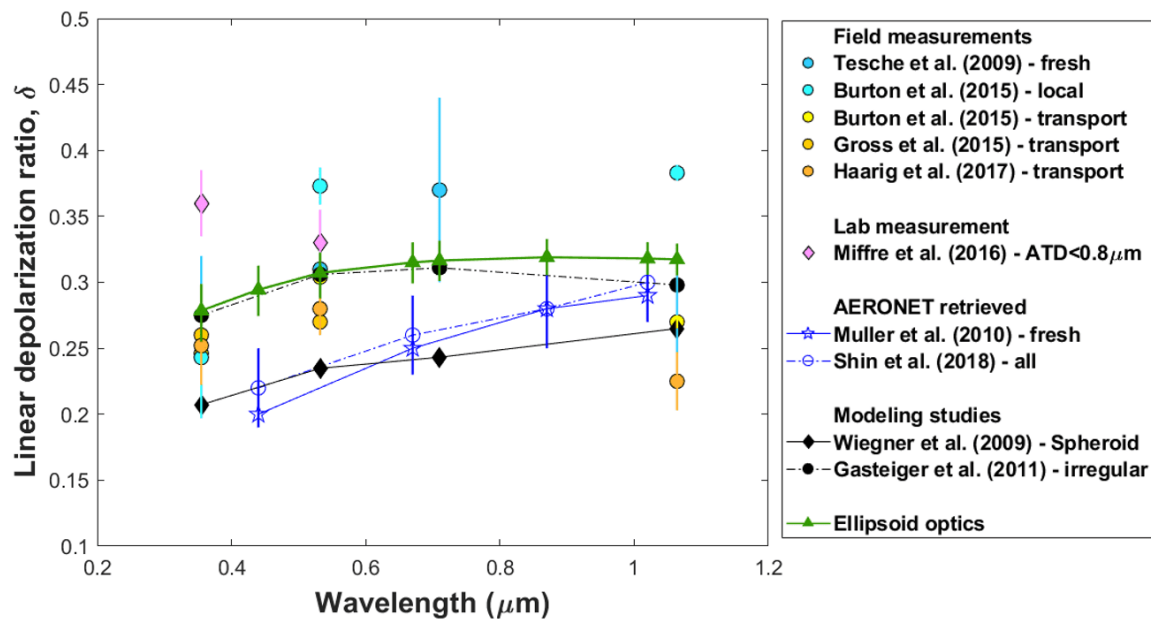
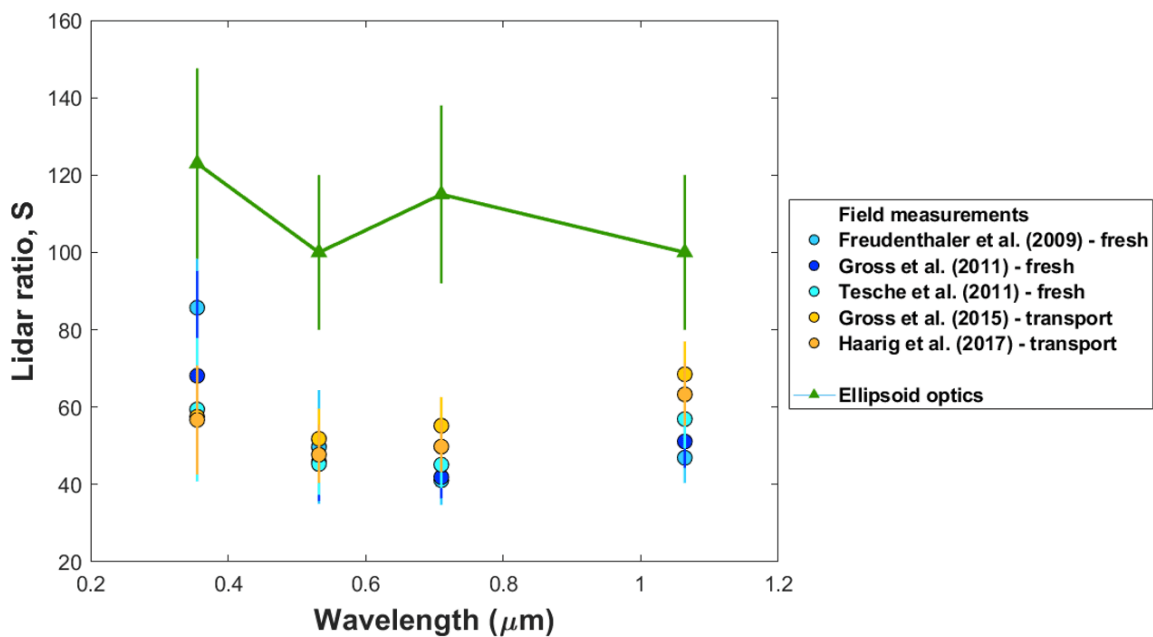


Figure 5. Root-mean-square errors between lab-measured and simulated  $\log_{10}(\frac{P_{11}(\theta)}{P_{11}(30^\circ)})$ ,  $-\frac{P_{12}(\theta)}{P_{11}(\theta)}$ , and  $\frac{P_{22}(\theta)}{P_{11}(\theta)}$  at forward-scattering, sideward-scattering,

and backward-scattering angles. The vertical error bars denote uncertainties from the dust refractive index. The ellipsoidal dust optics show excellent agreements with measured  $-\frac{P_{12}}{P_{11}}$  and  $\frac{P_{22}}{P_{11}}$  at all scattering angles than spherical and spheroidal dust optics. The ellipsoidal dust optics show an improved agreement with measured  $P_{11}$  at almost all scattering angles (except at backward-scattering angles at 441.6 nm) than spherical and spheroidal dust optics.



**Figure 6. Observed and simulated linear depolarization ratio at various wavelengths.** The size distribution of ellipsoidal dust optics is taken as the one from Adebisi and Kok (2020), which obtained dust size distribution constraints from joint observational-modeling-experimental analysis. The shape distribution of ellipsoidal dust optics comes from observational constraints (aka, [Eqs 1 and 2](#)). The ellipsoidal dust optics excellently reproduce the magnitude and the wavelength-dependency of the observed linear depolarization ratio, whereas AERONET retrievals assuming a spheroidal dust shape (Dubovik et al., 2006) cannot.



**Figure 7. Observed and simulated lidar ratio at various wavelengths.** The size distribution of ellipsoidal dust optics is taken as the one from Adebisi and Kok (2020), which obtained dust size distribution constraints from joint observational-modeling-experimental analysis. The shape distribution of ellipsoidal dust optics comes from observational constraints (aka, [Eqs 1 and 2](#)). The ellipsoidal dust optics overestimate the lidar ratio by a factor of ~2 relative to observations, because ellipsoidal dust optics underestimate the phase function at backscattering angles (see  $\frac{P_{11}(\theta)}{P_{11}(30^\circ)}$  in [Figs. 3 and 4](#)).



## DISCUSSIONS AND CONCLUSIONS:

- This work approximates dust as ellipsoidal particles (**Fig. 1**) with observationally constrained shape distribution (**Eqs. 1-2**) in obtaining dust single-scattering properties.
- Models approximate dust as spherical particles, underestimating the extinction efficiency, mass extinction efficiency, single-scattering albedo, and asymmetry factor at both shortwave and longwave spectra relative to ellipsoidal dust shape (**Fig. 2**).
  - This finding helps explain why models underestimate the light extinction per dust mass loading.
  - The look-up table of ellipsoidal dust optics has been applied to improve several global aerosol models, including Spanish MONARCH (Klose et al., 2021), Japanese IMPROVE (Ito et al., 2021), NCAR CESM (Meng et al., submitted to GRL), and NASA GISS ModelE (Huang et al., in prep.).
  - Investigation on the impacts of dust shape on the top-of-atmosphere and surface longwave and shortwave radiative forcings is ongoing.
- Ellipsoidal dust optics can reproduce the observed scattering matrix (**Figs. 3-5**) and observed linear depolarization ratio (**Fig. 6**) in a substantially improved way than spheroidal dust optics which are widely used in remote sensing retrievals. However, ellipsoidal dust optics overestimate the lidar ratio by a factor of ~2 relative to observations (**Fig. 7**).
  - This finding indicates that a realistic quantification of dust body shape is not sufficient enough at backscattering angles.
  - Accurate quantifications of dust surface texture (roughness, pits, and sharp corners) are further needed.

# ACKNOWLEDGMENTS AND REFERENCES

- Yue Huang acknowledges support from the Columbia University Earth Institute Postdoctoral Research Fellowship and the NASA grant number 80NSSC19K1346, awarded under the Future Investigators in NASA Earth and Space Science and Technology (FINESST) program.
- Jasper F. Kok acknowledges support by the NSF grants 1552519 and 1856389, and the Army Research Office under Cooperative Agreement Number W911NF-20-2-0150.
- Olga Muñoz acknowledges support from the excellence research program of the Andalusian Regional Government grant P18-RT-1854, the National Plan of Scientific and Technical Research and Innovation of the Spanish Ministry of Science and Innovation grant RTI2018-095330-B-I00 (LEONIDAS) and the "Center of Excellence Severo Ochoa" awarded to IAA-CSIC (SEV-2017-0709) by the Spanish State Agency for Research.
- The authors thank Oleg Dubovik for providing the Dubovik et al. (2006) kernel on the spheroidal dust optics, thank Ping Yang and Bingqi Yi for providing the Meng et al. (2010) database on the ellipsoidal dust optics, and thank Matthias Tesche for providing the Tesche et al. (2019) compilation on the observed linear depolarization ratio. In addition, the authors thank Masanori Saito, Ron Miller, Hongbin Yu, Longlei Li, Adeyemi Adebisi, Jun Meng, Pablo Saide, Marcelo Chamecki, Yu Gu, Yoshihide Takano, and the late Kuo-Nan Liou for insightful discussions.

## References:

- Adebisi, A. A., & Kok, J. F. (2020). Climate models miss most of the coarse dust in the atmosphere. *Science Advances*, 6(15), eaaz9507.
- Dubovik, O., Sinyuk, A., Lapyonok, T., Holben, B. N., Mishchenko, M., Yang, P., Eck, T. F., Volten, H., Muñoz, O., Veihelmann, B., van der Zande, W. J., Leon, J. F., Sorokin, M., & Slutsker, I. (2006). Application of spheroid models to account for aerosol particle nonsphericity in remote sensing of desert dust. *Journal of Geophysical Research Atmospheres*, 111(11), D11208.
- Huang, Y., Kok, J. F., Kandler, K., Lindqvist, H., Nousiainen, T., Sakai, T., Adebisi, A., & Jokinen, O. (2020). Climate models and remote sensing retrievals neglect substantial desert dust asphericity. *Geophysical Research Letters*, 47(6), 1–11.
- Kok, J. F., Ridley, D. A., Zhou, Q., Miller, R. L., Zhao, C., Heald, C. L., Ward, D. S., Albani, S., & Haustein, K. (2017). Smaller desert dust cooling effect estimated from analysis of dust size and abundance. *Nature Geoscience*, 10, 274–278.
- Meng, Z., Yang, P., Kattawar, G. W., Bi, L., Liou, K. N., & Laszlo, I. (2010). Single-scattering properties of tri-axial ellipsoidal mineral dust aerosols: A database for application to radiative transfer calculations. *Journal of Aerosol Science*, 41(5), 501–512.
- Tesche, M., Kolgotin, A., Haarig, M., Burton, S. P., Ferrare, R. A., Hostetler, C. A., & Müller, D. (2019). 3+2 + X: What is the most useful depolarization input for retrieving microphysical properties of non-spherical particles from lidar measurements using the spheroid model of Dubovik et al. (2006)? *Atmospheric Measurement Techniques*, 12(8), 4421–4437.
- Volten, H., Muñoz, O., Rol, E., de Haan, J. F., Vassen, W., Hovenier, J. W., Muinonen, K., & Nousiainen, T. (2001). Scattering matrices of mineral aerosol particles at 441.6 nm and 632.8 nm. *Journal of Geophysical Research*, 106(D15), 17375–17401.

## AUTHOR INFORMATION

Dr. Yue Huang ([yh3456@columbia.edu](mailto:yh3456@columbia.edu), [yue.huang@nasa.gov](mailto:yue.huang@nasa.gov)) is a climate scientist, who is interested in the role of atmospheric aerosols in climate change and mitigation. She is currently a postdoctoral research scholar at NASA GISS and Columbia University, advised by Dr. Ron L. Miller and funded by the Earth Institute postdoctoral fellowship (2021-2023 Fellow). She earned her Ph.D. (2015-2021) with [Professor Jasper F. Kok](https://jasperfkok.com/people/) (<https://jasperfkok.com/people/>) at the University of California Los Angeles on microphysical and optical properties of dust aerosols. Her doctoral research was funded by the NASA FINESST graduate fellowship (2019-2021 Fellow). You can find more information on her [website](https://huangyue.wixsite.com/mysite) (<https://huangyue.wixsite.com/mysite>).

## ABSTRACT

Accurate single-scattering properties of dust aerosols are critical to the global aerosol models and retrieval algorithms of remote sensing products to correctly simulate and retrieve dust distributions. However, inconsistent and inaccurate quantifications of dust shape exist, as almost all models approximate dust as spherical particles, whereas most retrieval algorithms approximate dust as spheroidal particles with an unrealistic shape distribution. These problematic shape quantifications can generate biases in the single-scattering properties that further propagate into the estimated dust distributions. Here, we obtain dust single-scattering properties by approximating dust as tri-axial ellipsoidal particles with observationally constrained shape distribution. We find that approximating dust as spherical particles and neglecting dust asphericity, as almost all models do, underestimate the extinction efficiency, mass extinction efficiency, asymmetry factor, and single-scattering albedo for all dust sizes at both shortwave and longwave spectra. We further find that approximating dust as spheroidal particles and underestimating dust asphericity, as most retrieval algorithms do, result in an incorrect magnitude and wavelength dependence of the linear depolarization ratio relative to observations. Conversely, approximating dust as ellipsoidal particles with observationally constrained shape distribution produces an excellent agreement with the measured linear depolarization ratio. Although the new ellipsoidal dust optics show potential to improve models and retrieval algorithms, it underestimates the magnitude of the backscattering intensity relative to observations. This indicates that a realistic quantification of dust body shape is not sufficient and that an accurate quantification of dust surface texture is also critical to accurately reproduce dust optics at backscattering angles.